# Residual Stress in Multi-indented Surface Layer of Partially Stabilized Zirconia Ceramics

Katsumi Mizutani[1], Kazuo Murata[2] and Yoshio Tanaka[3]

## Abstract

It is found that compressive residual stress of ground partially stabilized zirconia ceramics is remarkably higher than those of other ceramics. To clarify the causes of its high residual stress, multi-indentation, which is analogous to burnishing in grinding, on the surface of the material was carried out. Three kinds of methods to evaluate the residual stress were taken: X-ray stress measurement, an elastic-plastic indentation analysis, an estimation method based on fraction of phase transformation.

The result shows that ( 1 ) the residual stress can be predicted by the indentation analysis taking into account pressure hardening effect for yield compressive stress, and ( 2 ) the compressive residual stress due to phase transformation from tetragonal to monoclinic reaches about 65% of the total stress averaged in its existing depth.

## Introduction

Partially stabilized zirconia ceramics (PSZ) are used for the material of machine elements, food processing parts and artificial bones because of their high hardness, strength, and chemical stability. The ceramics are usually ground with diamond wheel after sintering process. The grinding shapes the surface of ceramics smooth but inevitably induces some changes in quality in the surface layer. Residual stress is a typical example of such changes in quality because it exerts large influence on strength and on shape accuracy of the ground ceramics. The surface residual stresses of ground ceramics have been measured using X-ray diffraction technique[1]. One of the remarkable results is that PSZ could have compressive surface stress several times larger than other ceramics[2]. Stress induced phase transformation from tetragonal to monoclinic is well recognized as a cause for this high compressive stress. Its transformation in the surface layer involves a volume increase to form compressive residual stress in it. Its quantitative findings, however, especially about the magnitude and depth of the compressive surface stress are few though they should be connected with material properties and grinding conditions. To clarify such nature on surface residual stress further, a model analogous to burnishing action of abrasive grain in grinding should be treated not only experimentally but also analytically. Its appropriate one must be the multi-indentation model.

This paper deals with the surface residual stress of PSZ multi-indented by Vickers indenter. Three kinds of residual stresses on the surface are compared: ( 1 ) experimentally measured by X-ray, ( 2 ) determined by elastic-plastic indentation

1 . Department of Mechanical Engineering, Kinki University, Wakayama 649-6493, Japan
2 . Technology Research Institute of Osaka Prefecture, Osaka 594-1157, Japan
3 . Department of Mechanical Engineering, Osaka Prefecture University, Osaka 599-8531, Japan

analysis, (3) estimated from the volume expansion due to the phase transformation. The proportion of the residual stress due to the transformation to the total residual stress is also clarified.

## Method for Determining Residual Stress on Multi-indented Surface

### I. Multi-indentation Model

It is well known that the residual stress of a free body is due to the plastic deformation partially induced in the body. Consider the plastic deformation of work ceramics in material removal process of grinding, for the mechanism of residual stress formation in the surface layer of ground PSZ. Figure 1 illustrates a typical behavior of work material along the path of an abrasive grain on a wheel. As increase in the grain depth of cut, work material is deformed plastically without material removal (burnishing), removed with flow type chip (flow type removal), and removed with fracture type chip (fracture type removal). To estimate the shares exposed by burnishing, by flow type removal, and by fracture type removal, specific grinding energy U and ratio of tangential force to normal force $F_t/F_n$ were measured in grinding of PSZ and SK5 (tool steel, which does not include fracture type removal)[3]. Specific grinding energy normalized by hardness U/Hv was 6 in PSZ and 30 in SK5 under the standard grinding condition. The $F_t/F_n$ was 0.1 in PSZ and 0.5 in SK5. These results show that plastic deformation in grinding of PZT comes mainly from burnishing (smaller $F_t/F_n$ in PSZ), though its share in the grinding process is relatively low being limited by fracture type removal (smaller U/Hv in PSZ). Then, residual stress formation in grinding is analogous to that in depressing with indenters. Figure 2 illustrates the analogy between grinding and multi-indentation in respect of residual stress formation. The burnishing by grain in (a) is replaced by the indentation in (b). Burnishing interval which depend mainly on the fracture scale is treated as indenter interval L, and both grain size and grain depth of cut as depression size. We use this multi-indentation model to analyze residual stress in the surface layer of PSZ instead of dealing with the complicated process shown in Fig. 1.
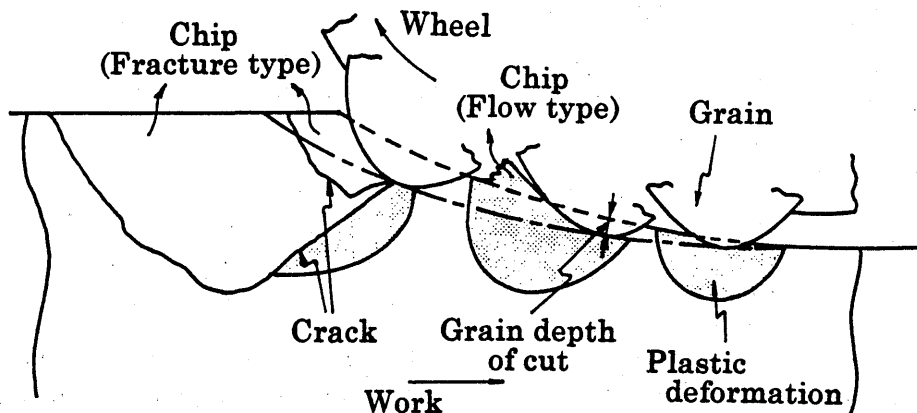


Figure 1. Schematic illustration showing typical deformation and fracture of ceramics in a material removal process of grinding.
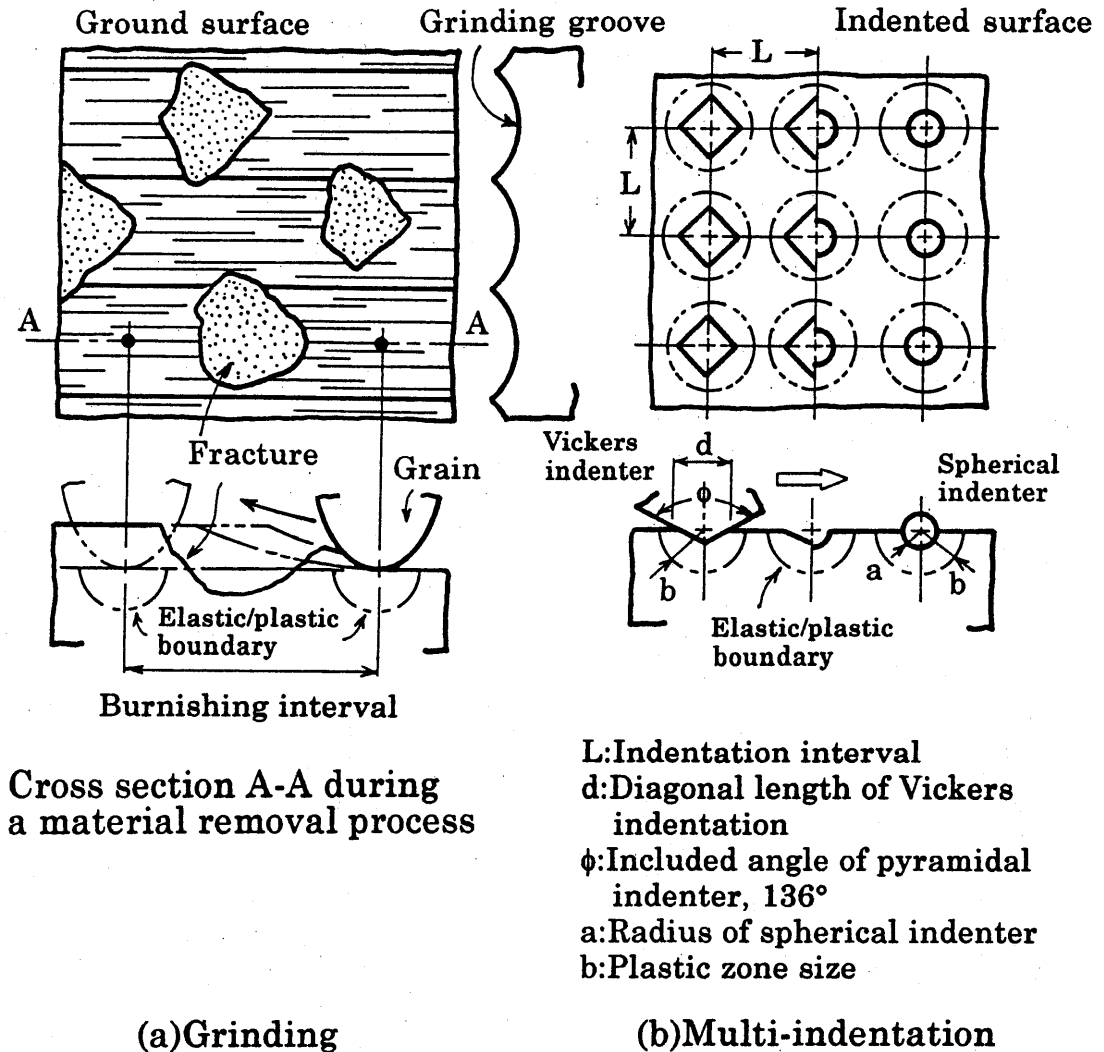
Ground surface    Grinding groove    Indented surface

Fracture    Grain    Vickers indenter    Spherical indenter

Elastic/plastic boundary    Elastic/plastic boundary

Burnishing interval

**Cross section A-A during a material removal process**

L:Indentation interval
d:Diagonal length of Vickers indentation
φ:Included angle of pyramidal indenter, 136°
a:Radius of spherical indenter
b:Plastic zone size

**(a)Grinding**    **(b)Multi-indentation**

Figure 2. An analogy between grinding and multi-indentation in respect of residual stress formation.

## II. Multi-indentation Procedure

PSZ used here is 3 mol% yttria-doped tetragonal zirconia polycrystals with average grain size of $0.5 \mu$m. Table 1 shows, mechanical properties of this material. The size of the specimen is 8 by 8 by 4 mm. In the experiment, Vickers indentations were carried out on a surface of the specimen polished with $0.25 \mu$m-grit diamond powder: the surface consists of tetragonal phase until indentation. Conditions for the multi-indentation are $L=50 \mu$m, $80 \mu$m, $100 \mu$m, $150 \mu$m and $200 \mu$m, indentation load $P=10$N.

Table 1. Mechanical properties of PSZ used.

| Young's modulus | $2.06 \times 10^5$ MPa |
|---|---|
| Poisson's ratio | 0.31 |
| Vickers hardness | $14 \times 10^3$ MPa |
| Bending strength | $1.2 \times 10^3$ MPa |
| Fracture toughness | 9 MN/m$^{3/2}$ |

## III. Method for Evaluating the Residual Stress

(1) X-ray Stress Measurement

This measurement follows $\sin^2 \phi$ method. Table 2 shows condition of X-ray diffraction using parallel beam. The Bragg angle $\theta$ was measured under $\phi = 0°$, 15°, 30° and 45° (tilt angle for the specimen), then the residual stress was determined by the following equation[1].

Table 2. Conditions of X-ray stress measurement.

| Characteristic X-ray | CrK$\alpha$ |
|---|---|
| Diffraction plane | (133) |
| Diffraction angle | 152.69° |
| Filter | V |
| Irradiated area | $4 \times 8$ mm$^2$ |
| Tube voltage | 30 kV |
| Tube current | 10 mA |
| Divergent angle | 1.0° |
| Time constant | 5 sec |

$$\sigma = -\frac{E}{2(1+v)} \cot \theta_0 \frac{\pi}{180} M \qquad (1)$$

where, M is the gradient in $2\theta$-$\sin^2 \phi$ diagram, E the Young's modulus, $\nu$ the Poisson's ratio and $\theta_0$ the Bragg angle for the stress-free state.
Effective penetration depth of Cr-K$\alpha$ X-ray is $2.6 \mu$m($\phi = 0°$), $1.3 \mu$m ($\phi = 45°$) for PSZ.

(2) Elastic-plastic Indentation Analysis

Chiang et al.[4] presented an approach for the stress field of a hemi-spherical method to the residual stress in multi-indented surface layer. Our method contains three steps. The first is replacing the Vickers indentation with the hemi-spherical one as shown in fig. 2 (b). This replacement implies the agreement that ( 1 ) the plastic zones of both indentations expand as hemispheres with same radius when the depression volumes are the same ($a=0.225d$), and ( 2 ) the stresses in both cases are equal except the zone close to the depression. The second is calculating the residual stress after unloading process (elastic deformation) which follows loading process (elastic-plastic deformation) of hemi-spherical indentation. Figure 3 shows the procedure. A stress at a point below $\Box 0ABC$ is determined by superposing the stresses from each indentations. These stresses in a thin layer at depth $\zeta$ are averaged as the residual stress $\sigma_p$ which has profile shown in fig. 3 . The third is taking the weighted average of $\sigma_p$ by considering X-ray absorption effect in terms of depth, to evaluate the residual stress that is comparable to one measured by X-ray method. This stress $\sigma_{pe}$, named as equivalent surface residual stress from indentation analysis, is given by
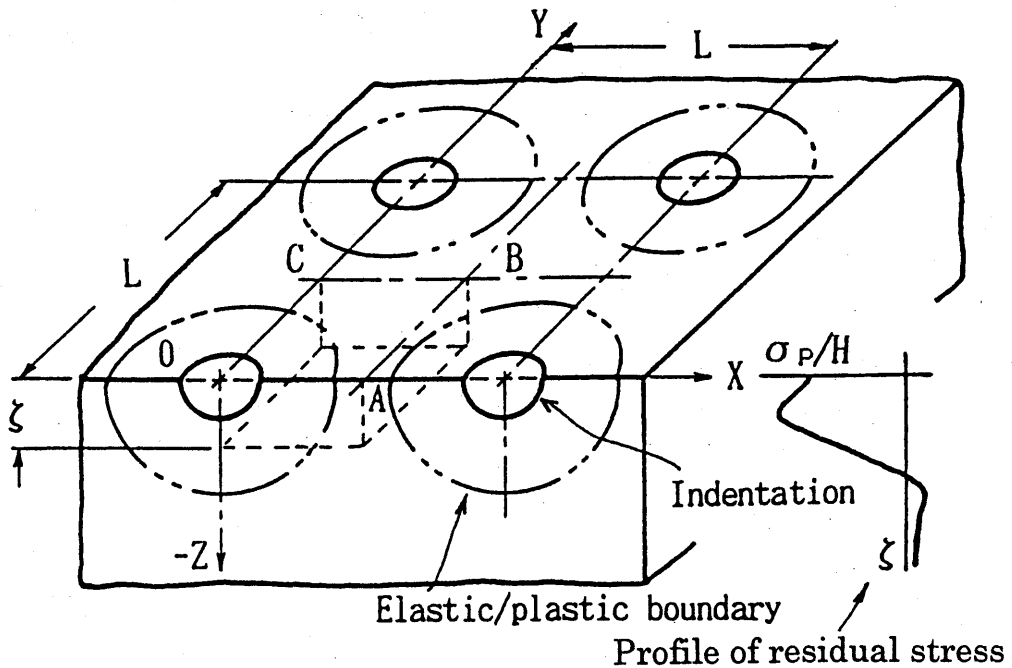


Figure 3 . An illustration for stress analysis in multi-indentation.

$$\sigma_{pe} = \frac{\int_0^{T/a} \sigma_P(\zeta)e^{-\mu Ba\zeta}\, d\zeta}{\int_o^{T/a} e^{-\mu Ba\zeta}\, d\zeta}$$

(2)

$$B = 1/\sin\theta_i + 1/\sin(2\theta_o - \theta_i)$$

where, $\zeta$ is the dimensionless depth normalized by a, T the penetration depth of X-ray, $\mu$ the linear absorption coefficient, $\theta_i$ the X-ray incident angle. All the things needed to determine $\sigma_{pe}$ are radius of hemi-spherical indentation a(=0.225d), indentation interval L, Poisson's ratio $\nu$, relative plastic zone size $\beta$(=b/a). In many ceramics, $\beta$ is approximately given by[5]

$$\beta = 0.83(E/Hv)^{2/5} \tag{3}$$

where, Hv is the Vickers hardness, E the Young's modulus.

For the material exhibiting transformation plasticity like PSZ, Chen[6] demonstrated that the compressive yield stress Y is pressure dependent by suffering shear and dilatation effects. That is

$$Y = Y_0 + \alpha P \tag{4}$$

where, $Y_0$ is Y at zero pressure, $\alpha$ the coefficient of pressure hardening, P the hydraulic pressure. In this case, $\beta$ can be calculated by using $\alpha$, Hv, E, and $\nu$.

(3) Estimation Based on Volume Expansion due to Phase Transformation

When the layer parallel to the surface in a large body of PZT suffers a volume increase due to transformation of tetragonal to monoclinic, the biaxial compressive stress in this layer can be calculated by[7]

$$\sigma_m(x) = E\gamma C_m(x)/(1-v) \tag{5}$$

where, x is the depth from surface, $\sigma_m(x)$ the residual stress due to the transformation at depth x, $\gamma$ the linear expansion coefficient for the volume increase, $C_m(x)$ the volume fraction of monoclinic phase newly developed at depth x. If the lattice constants of tetragonal and monoclinic phase are known, $\gamma$ can be easily calculated under the isotropic volume increase. The X-ray diffraction profile for PSZ used here indicated that the interplanar spacings of tetragonal and monoclinic phase were equivalent to those from No.14-534 and No. 7-343 in JCPDS, respectively. Then, a=5.09Å and c=5.18Å in tetragonal phase, a=5.143Å, b=5.204Å, c=5.311Å and $\beta$=80.75° in monoclinic phase[8]. After calculating, $\gamma \doteqdot 0.015$.

For determining $C_m(x)$, a thin film X-ray diffraction at an angle of incident X-ray ($a = 1°$) was utilized on the surface stepwise removed by polishing. Since the diffraction of $a = 1°$ treats just in the thin surface layer, this repeated measurement on the surface stepwise removed can give a distribution comparable to $C_m(x)$. The distribution $C_m(x)$ is estimated using measured data of diffracted intensities from monoclinic (11$\bar{1}$), (111) and tetragonal (111) as follows[9].

$$C_m(x) = \frac{I_m(11\bar{1}) + I_m(111)}{I_t(111) + I_m(11\bar{1}) + I_m(111)} \tag{6}$$

The estimated stress $\sigma_m(x)$ is also averaged by the same manner in Eq.(2) as equivalent surface residual stress due to phase transformation $\sigma_{me}$.

## Results and discussion

The compressive surface residual stresses obtained by both X-ray measurement and indentation analysis are compared in Fig. 4 . The measured stress $\sigma/\mathrm{Hv}$ locates between the two of $\sigma_{pe}/\mathrm{H}$ calculated. One of the calculated is of relative plastic zone size $\beta = 2.43$ ($\alpha = 0$) given by Eq.(3). This indicates $\sigma_{pe}/\mathrm{H} = 0.85$ $\sigma/\mathrm{Hv}$, though $\sigma_{pe}/\mathrm{H} = \sigma/\mathrm{Hv}$ for the material without transformation plasticity, $Si_3N_4$, $Al_2O_3$, and $SiC$[5]. The other is of $\beta = 4.64$ ($\alpha = 2$, which is quoted from data by Chen[6]) as the case of pressure hardening compressive yield stress. This indicates $\sigma_{pe}/\mathrm{H} = 1.4 \sigma/\mathrm{Hv}$. For PSZ used here, $\alpha = 0$ is underestimated and $\alpha = 2$ overestimated. We do not have our data on $\alpha$. If allowed to select $\alpha$ arbitrary, $\alpha = 0.5$, consequently $\beta = 3.28$ could indicate good agreement between $\sigma/\mathrm{Hv}$ and $\sigma_{pe}/\mathrm{H}$.
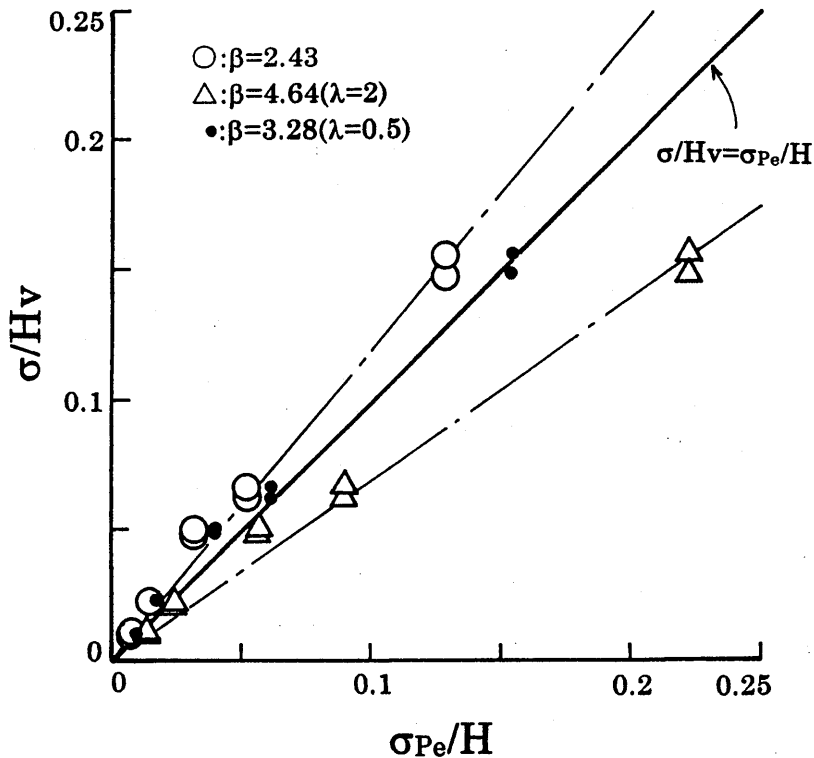


Figure 4 . Relation between measured compressive residual stress
$\sigma/\mathrm{Hv}$ and analyzed compressive residual stress $\sigma_{pe}/\mathrm{H}$.

This agreement will lead to the prediction of the residual stress by the indentation analysis, which is easy to discuss its conditions affecting the residual stress. Figure 5 shows relationship among compressive residual stress $\sigma/\mathrm{Hv}$, $\sigma_{pe}/\mathrm{H}$ and indentation interval $L/a$. Compressive residual stress steeply increases as indentation interval decreases. This relation explains one reason on higher compressive residual stress of ground PSZ than other ceramics, because small size fracture of PSZ in grinding corresponds to smaller $L/a$.
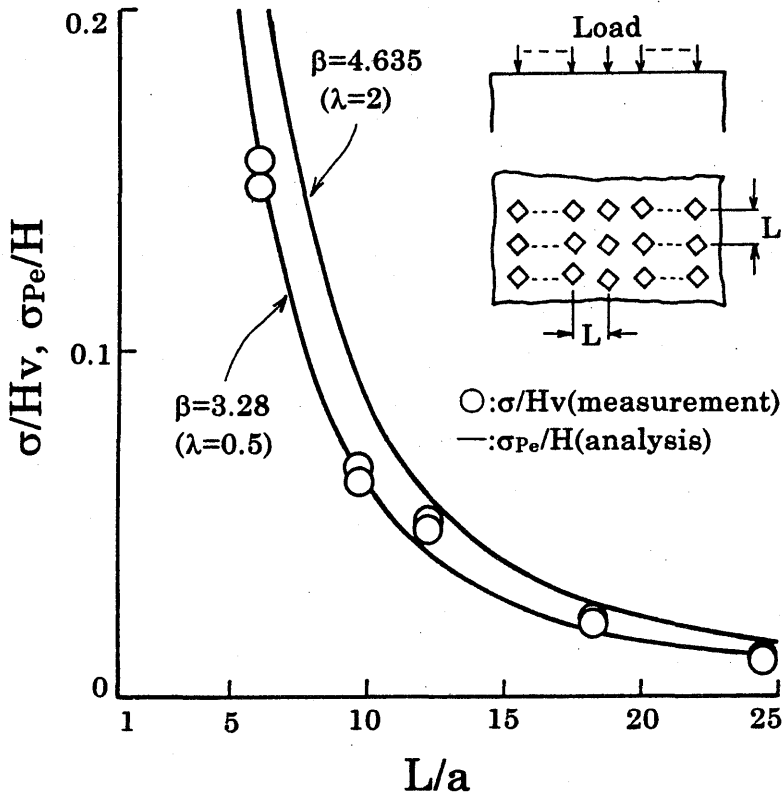
Figure 5. Relation among normalized compressive residual stress
$\sigma$/Hv (measured), $\sigma_{pe}$/H (analyzed), and indentation
interval normalized by equivalent spherical radius L/a.

The compressive residual stress $\sigma$ consists of complex effect from both plastic deformation of tetragonal phase and deformation by phase transformation. For realizing the nature of the deformation, it is effective to compare $\sigma$ with $\sigma_{me}$ induced by the phase transformation, as shown in Fig. 6. The stress $\sigma_{me}$ accounts for large part of $\sigma : \sigma_{me}/\sigma = 0.66$ averaged in $x \leqq 12\mu$m. It is also notable that $\sigma_{me}$ disappears in $x > 15\mu$m, though $\sigma$ still holds some values and the half-value breath for tetragonal phase decreases even in $x > 15\mu$m. Then, it seems that critical condition for plastic deformation of tetragonal phase is lower than for the phase transformation, and the plastic deformation is expanded by the stress field due to the transformation. This expanded plastic deformation must causes increase in $\beta$ from 2.43 to 3.28 in this indentation analysis.
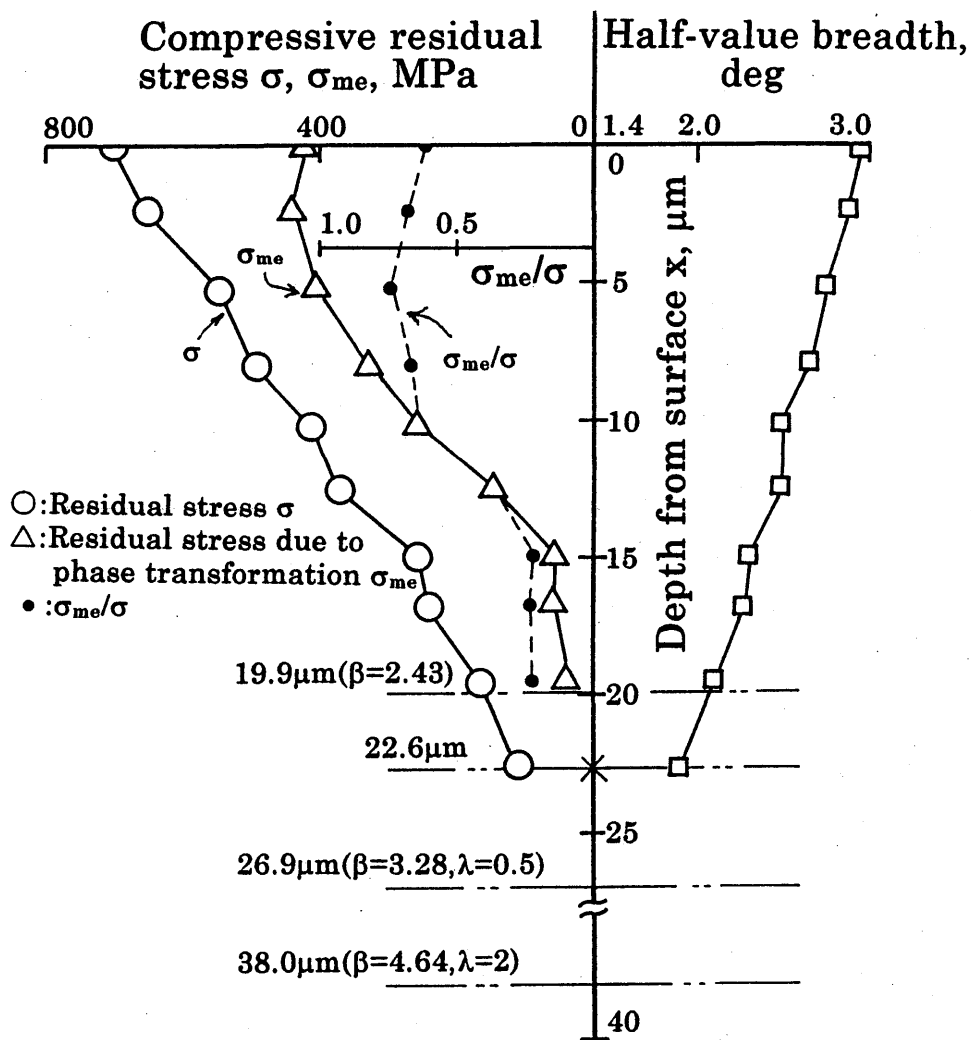
Figure 6. Depth dependent distribution of compressive residual stress $\sigma$, equivalent compressive residual stress due to phase transformation $\sigma_{me}$, and half value breadth of X-ray diffraction profile.

## Conclusion

Compressive residual stress on the surface of PSZ multi-indented was evaluated by three kinds of methods. Followings are clarified.

(1) The compressive residual stress $\sigma$ can be approximately estimated by a elastic-plastic indentation analysis that takes pressure hardening effect for compressive yield stress into account.

(2) The residual stress due to the phase transformation $\sigma_{me}$ reaches about 65% of $\sigma$ in its existing depth

(3) Plastic deformation of tetragonal phase exists in the depth deeper than existing depth of $\sigma_{me}$.

## References

(1) K. Tanaka, (1987), X-ray stress measurement, Proc. of the 24th workshop on X-ray studies of mechanical behavior of material (in Japanese), 1-7.

(2) K. Tanaka, T. Kurimura, and Y. Akiniwa, (1987), X-ray stress measurement of ground surface of partially stabilized zirconia (Y-TZP), Proc. of the 24th symposium an X-ray studies on mechanical behavior of material (in Japanese), 214-218.

(3) K. Mizutani and K. Murata, (1992), Residual stress in ground surface of ceramics.
In: Progress of cutting and grinding vol. I. (D. Chen and N. Narutaki eds) p175-180, International Academic Publishers, Beijing.

(4) S.S.Chiang, D.B.Marshall, and A.G. Evans, (1982), The response of solids to elastic/plastic indentation: I. Stresses and residual stresses, J.Appl.Phys., 53,298-311.

(5) K. Murata, K., Mizutani, and Y. Tanaka, (1994), Residual stress in multi-indented surface layer of ceramics-effects of hardness and X-ray penetration depth on residual stress (in Japanese), J. Soc. Mater. Sci., Japan, 43, 772-778.

(6) I. Chen, (1986), Implications of transformation plasticity in $ZrO_2$-containing ceramics: II, Elastic-plastic indentation, J. Am. Ceram. Soc., 69, 189-194.

(7) K. Mizutani, K. Murata, and Y. Tanaka, (1989), Residual stress and bent deformation induced by grinding of thin plate of Y-TZP (in Japanese), J. Jpn. Soc. Prec. Eng., 55, 703-708.

(8) Index to the X-ray data file (No. 14-534, No. 7-343), American society standards for testing and materials, Compiled by joint committee on powder diffraction standards.

(9) R. Garvie and P. Nicholson, (1972), Phase analysis in zirconia systems, J. Am. Ceram. Soc. 55, 303-305.

**和文抄録**

多数圧子押込みされた部分安定化ジルコニアセラミックス表面層の残留応力

水谷勝己, 村田一夫, 田中芳雄

　部分安定化ジルコニアセラミックスは高い硬度と強度、耐食性などのため機械構造材料、食品加工部材、生体材料などに利用されている。それらは、焼結後に研削加工が施され良好な表面に仕上げられるが、その際に生じる残留応力などの加工変質が部品の強度や精度に大きな影響を与えるものとなっている。

　本研究では、応力誘起の相変態を生じるこの材料に対する研削残留応力の大きさと深さの予測を目的として、研削時の残留応力生成機構をモデル化した多数ビッカース圧子押込みを材料表面に対して行っている。多数圧子押込み面の残留応力を①X線解析によって実験的に測定する、②押込みの弾塑性応力解析から推定する、③応力誘起の相変態による体積膨脹から推定することを行い、それぞれを比較検討した結果、以下のことが明らかになった。

（１）その残留応力は、押込み条件と材料特性を与えたとき、圧縮降伏応力の圧力硬化を考慮した弾塑性の応力解析により概略推定することが出来る。

（２）相変態による残留応力の全体に対する寄与は約65％である。残りは正方晶の塑性変形によるもので、相変態によるものより深くまで存在している。